

C–H bond activation through steric crowding of normally inert ligands in the sterically crowded gadolinium and yttrium $(C_5Me_5)_3M$ complexes

William J. Evans*, Benjamin L. Davis, Timothy M. Champagne, and Joseph W. Ziller

Department of Chemistry, University of California, Irvine, CA 92697-2025

Edited by Harry B. Gray, California Institute of Technology, Pasadena, CA, and approved June 26, 2006 (received for review April 5, 2006)

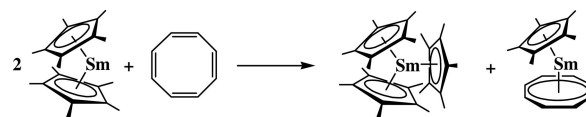
Synthesis of the sterically crowded Tris(pentamethylcyclopentadienyl) lanthanide complexes, $(C_5Me_5)_3Ln$, has demonstrated that organometallic complexes with unconventionally long metal ligand bond lengths can be isolated that provide options to develop new types of ligand reactivity based on steric crowding. Previously, the $(C_5Me_5)_3M$ complexes were known only with the larger lanthanides, La–Sm. The synthesis of even more crowded complexes of the smaller metals Gd and Y is reported here. These complexes allow an evaluation of the size/reactivity correlations previously limited to the larger metals and demonstrate a previously undescribed type of C_5Me_5 -based reaction, namely C–H bond activation. $(C_5Me_5)_3Gd$, was prepared from $GdCl_3$ through $(C_5Me_5)_2GdCl_2K(THF)_2$, $(C_5Me_5)_2Gd(C_3H_5)$, and $[(C_5Me_5)_2Gd][BPh_4]$ and structurally characterized by x-ray crystallography. Although Gd^{3+} is redox-inactive, $(C_5Me_5)_3Gd$ functions as a reducing agent in reactions with 1,3,5,7-cyclooctatetraene (COT) and triphenylphosphine selenide to make $(C_5Me_5)_2Gd(C_8H_8)$, $[(C_5Me_5)_2Gd]_2Se_2$, and $[(C_5Me_5)_2Gd]_2Se$ depending on the stoichiometry used. When the analogous synthetic method was attempted with yttrium in arene solvents, the previously characterized $(C_5Me_5)_2YR$ complexes ($R=C_6H_5$, $CH_2C_6H_5$) were isolated instead, i.e., C–H bond activation of solvent occurred. To avoid this problem, $(C_5Me_5)_3Y$ was synthesized in high yield from $[(C_5Me_5)_2YH]_2$ and tetramethylfulvene in aliphatic solvents. Isolated $(C_5Me_5)_3Y$ was found to metalate benzene and toluene with concomitant formation of C_5Me_5H , a reaction contrary to the normal pK_a values of these hydrocarbons. In this case, the normally inert $(C_5Me_5)^{1-}$ ligand engages in C–H bond activation due to the extreme steric crowding.

sterically induced reduction | lanthanide | pentamethylcyclopentadienyl | arene activation | long-bond organometallics

The pentamethylcyclopentadienyl ligand, $(C_5Me_5)^{1-}$, has been an important component of numerous classes of organometallic complexes providing stability, solubility, and crystallinity to more reactive metal ligand moieties. $(C_5Me_5)^{1-}$ functions predominately as an ancillary spectator ligand that does not become involved in organometallic reaction pathways. One or two of these ligands are typically found in organometallic complexes, but not three because the cone angle of a $(C_5Me_5)^{1-}$ ligand was estimated to be as large as 142° (1), and, as a consequence, the formation of $(C_5Me_5)_3M$ complexes was presumed to be impossible.

Recent developments in the organometallic chemistry of the f elements have shown that it is possible to isolate an entire series of $(C_5Me_5)_3M$ complexes in which the M–C bond distances are longer than conventional bond lengths (2). The ligands in these so-called long-bond organometallic complexes display different patterns of reactivity because they are not in a bonding arrangement that gives them their usual amount of stabilization.

This phenomenon was first demonstrated with the Tris(pentamethylcyclopentadienyl) samarium complex, $(C_5Me_5)_3Sm$ (3), prepared according to Scheme 1. The structure of $(C_5Me_5)_3Sm$ was surprising in that it had a 120° rather than 142° cone angle. In $(C_5Me_5)_3Sm$, the $(C_5Me_5)^{1-}$ ligands can adopt a 120° cone angle because these ligands are further away from the metal center than



Scheme 1.

in normal trivalent samarium pentamethylcyclopentadienyl complexes (4).

Consistent with the unusual structural features in $(C_5Me_5)_3Sm$, this complex displayed chemistry that was abnormal for trivalent $(C_5Me_5)^{1-}$ lanthanide complexes (2, 5–8). In particular, the $(C_5Me_5)^{1-}$ ligand became activated and was no longer an inert ancillary ligand. Two main types of reactivity were initially identified (Scheme 2): (i) alkyl-like reactivity in which one of the $(C_5Me_5)^{1-}$ rings functioned as if it were η^1 -bonded in a $(C_5Me_5)_2Sm(\eta^1-C_5Me_5)$ complex and (ii) formal one-electron reduction chemistry in which one of the $(C_5Me_5)^{1-}$ ligands functioned as a reductant to give chemistry like that of divalent $(C_5Me_5)_2Sm$ (9–12). Both modes of reactivity apparently derived from the steric crowding in the molecule, and the reductive chemistry was accordingly called sterically induced reduction (SIR) (2, 10). These reactions demonstrated that the reactivity of a normally inert ancillary ligand, in this case $(C_5Me_5)^{1-}$, can be substantially modified by creating a coordination environment in which the ligands have unusually long bonds.

The opportunity to accomplish one-electron reduction chemistry like that of divalent $(C_5Me_5)_2Sm$ with a trivalent lanthanide complex suggested that size optimization of Sm(II)-like reductive chemistry would be possible if $(C_5Me_5)_3Ln$ complexes could be made across the series (2, 10–14). Size optimization of reactivity is a hallmark of the trivalent lanthanides: The metal with the ideal radial size for a particular reaction can be selected from 15 options (excluding radioactive Pm but including the chemically similar Y) that can vary from Lu (1.03-Å nine-coordinate radius) to La (1.21 Å) in ≈ 0.015 Å per metal increments (15). This goal is not possible with the known molecular divalent lanthanides, because the six examples known, although different in radial size, also differ significantly in reduction potential and reactivity (12, 16). Although Sm(II) has effectively provided new reductive reaction chemistry to the lanthanides with many types of substrates (11, 12, 16), there are also many reactions that did not give isolable products, perhaps because the size of the metal was not optimum.

Conflict of interest statement: No conflicts declared.

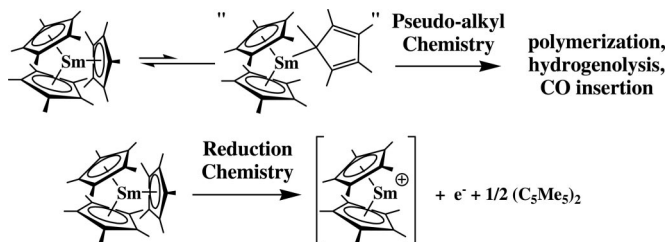
This paper was submitted directly (Track II) to the PNAS office.

Abbreviations: SIR, sterically induced reduction; TMF, tetramethylfulvene.

Data deposition: The atomic coordinates have been deposited in the Cambridge Structural Database, Cambridge Crystallographic Data Centre, Cambridge CB2 1EZ, United Kingdom (CSD reference nos. 603218–603223).

*To whom correspondence should be addressed. E-mail: wevans@uci.edu.

© 2006 by The National Academy of Sciences of the USA



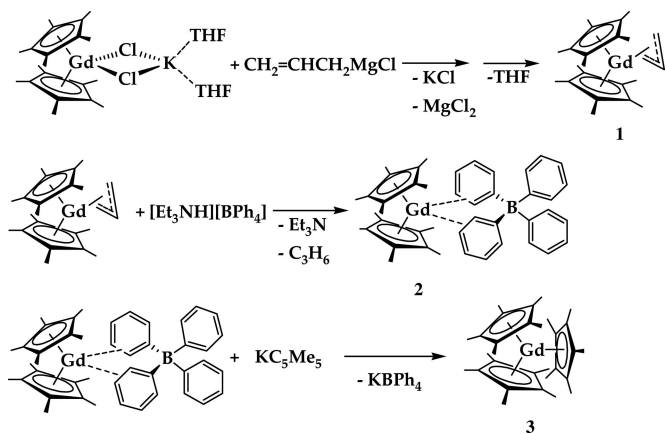
Scheme 2. Two general modes of reactivity for $(C_5Me_5)_3Sm$.

To test these ideas, the synthesis of other $(C_5Me_5)_3Ln$ complexes was necessary. Such syntheses required developing reactions that did not depend on the Sm(II) reactivity shown in Scheme 1. Successful syntheses of $(C_5Me_5)_3Ln$ complexes of the larger metals, La (1.216 Å) (17), Ce (1.196 Å) (8), Pr (1.179 Å) (8), and Nd (1.163 Å) (18) [compare Sm (1.132 Å)] were developed and provided $(C_5Me_5)_3Ln$ complexes slightly less sterically crowded than $(C_5Me_5)_3Sm$. Consistent with their reduced steric crowding, they are less reactive than $(C_5Me_5)_3Sm$, although they still are sterically crowded enough to participate in $(C_5Me_5)_2Ln(\eta^1-C_5Me_5)$ and SIR chemistry (8).

A more difficult synthetic challenge was to make $(C_5Me_5)_3Ln$ complexes of the metals smaller than Sm. These complexes would be more sterically crowded and presumably more reactive. Because the synthesis of some of the less crowded complexes had proven difficult, e.g., $(C_5Me_5)_3La$, $(C_5Me_5)_3Ce$, and $(C_5Me_5)_3Pr$ required the use of silylated glassware for isolation (8, 17), it was uncertain whether more crowded, presumably more reactive $(C_5Me_5)_3Ln$ complexes could be made. The next smaller metal, Eu, was not an alternative because Eu(III) is reported to be reduced by $(C_5Me_5)^{1-}$ and would not be expected to be stable (19). The next available lanthanide, Gd (1.107 Å), has a magnetic moment of $7.9 \mu_B$, which meant that all of the synthetic chemistry had to be done without any NMR spectroscopic analysis. Despite these difficulties, we report here the synthesis of $(C_5Me_5)_3Gd$. Among the next smallest members of the lanthanide-like metals, the most desirable was yttrium because it is diamagnetic. Although not formally a lanthanide, the $d^0 f^0 Y^{3+}$ ion behaves like the late lanthanides of similar size, holmium and erbium. Despite the small size of Y (1.075 Å), a $(C_5Me_5)_3Y$ complex can be isolated, and in so doing, a previously undescribed mode of $(C_5Me_5)^{1-}$ reactivity was identified.

Results

Synthesis of $(C_5Me_5)_3Gd$. The synthesis of $(C_5Me_5)_3Gd$ was attempted in analogous fashion to the successful syntheses of $(C_5Me_5)_3Ln$ [where Ln is La (18), Ce (8), Pr (8), Nd (18), or Sm (3)].



Scheme 3. The synthesis of $(C_5Me_5)_3Gd$.

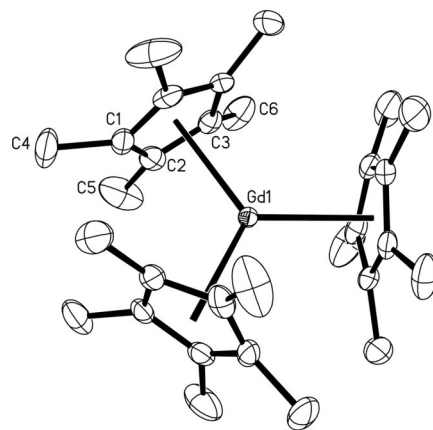


Fig. 1. Thermal ellipsoid plot of $(C_5Me_5)_3Gd$, **3**, with ellipsoids drawn at the 50% probability level.

Fortunately, the same synthetic steps generated $(C_5Me_5)_2Gd(C_3H_5)$, **1**, and $[(C_5Me_5)_2Gd][BPh_4]$, **2**, which were characterized by IR spectroscopy, elemental analysis, and their reaction chemistry (Scheme 3). Reaction of **2** with KC_5Me_5 formed $(C_5Me_5)_3Gd$, **3** (Fig. 1), an example of a $(C_5Me_5)_3M$ complex where M is smaller than Sm. To achieve good yields, however, it was essential to recrystallize **2** immediately before use and to use silylated glassware. The identity of $(C_5Me_5)_3Gd$ was established by x-ray crystallography (see Tables 1–3 and also Tables 4–6, which are published as supporting information on the PNAS web site).

Attempted Synthesis of $(C_5Me_5)_3Y$ via $[(C_5Me_5)_2Y][(\mu-Ph)_2BPh_2]$. Following the synthetic steps used in the synthesis of $(C_5Me_5)_3Gd$, $[(C_5Me_5)_2Y][(\mu-Ph)_2BPh_2]$, **4**, was synthesized in good yield and characterized by IR and NMR spectroscopy and x-ray crystallography (Fig. 2).

The yttrium metal center is formally eight coordinate, and the complex is isomorphous with $[(C_5Me_5)_2Sm][(\mu-Ph)_2BPh_2]$. As shown in Table 2, the complex has similar metrical parameters taking into account the 0.06-Å difference in ionic radii (15).

When $[(C_5Me_5)_2Y][(\mu-Ph)_2BPh_2]$ was reacted with KC_5Me_5 in benzene, an orange slurry formed. After the insoluble products were separated by centrifugation and the solvent was removed under vacuum, the 1H NMR spectrum in C_6D_{12} was consistent with that reported for $(C_5Me_5)_2Y(C_6H_5)$ (20) along with C_5Me_5H . When **4** was treated with KC_5Me_5 in toluene, a spectrum consistent with that reported for $(C_5Me_5)_2Y(CH_2C_6H_5)$ (20) and C_5Me_5H was observed (Fig. 3). Attempts to crystallize either of these products only afforded small amounts of crystals, some of which were identified as $[(C_5Me_5)_2Y]_2(\mu-O)$ by x-ray diffraction analysis (21).

Synthesis of $(C_5Me_5)_3Y$. The previous results showed that $[(C_5Me_5)_2Y][(\mu-Ph)_2BPh_2]$ was consumed in the reaction with KC_5Me_5 , but the product apparently metalated the arene used as solvent. These results suggested that the synthesis of $(C_5Me_5)_3Y$ required aliphatic solvents. Given the low solubility of KC_5Me_5 and $[(C_5Me_5)_2Y][(\mu-Ph)_2BPh_2]$ in aliphatic solvents, an alternative

Table 1. Selected bond distances (Å) and angles (°)

Parameter	$(C_5Me_5)_3Gd$, 3	$(C_5Me_5)_3Y$, 5
Ln(1)–Cnt	2.535	2.505
Ln(1)–C(1)	2.897 (4)	2.884 (3)
Ln(1)–C(2)	2.797 (2)	2.776 (2)
Ln(1)–C(3)	2.766 (2)	2.725 (2)
Cnt(1)–Ln(1)–Cnt(2)	120.0	120.0

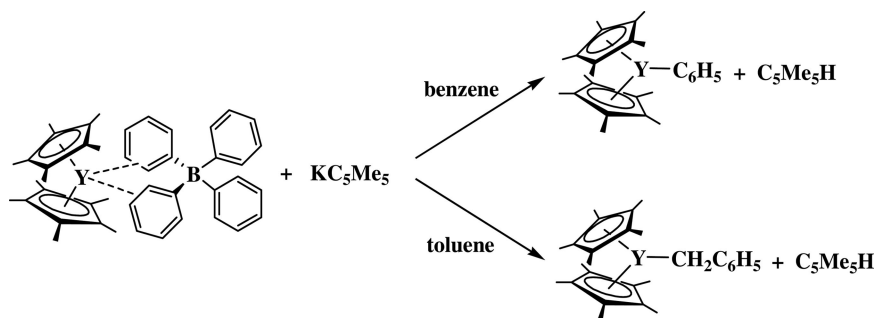


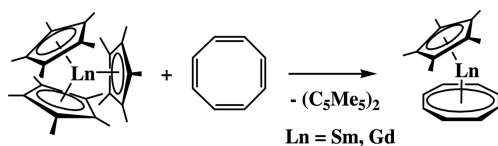
Fig. 3. Attempted synthesis of $(C_5Me_5)_3Y$ via $[(C_5Me_5)_2Y][(\mu-Ph)_2BPh_2]$.

Structure. The structures of $(C_5Me_5)_3Gd$ and $(C_5Me_5)_3Y$ suggest that the limit of steric crowding in $(C_5Me_5)_3Ln$ complexes has not been reached. As the most crowded of the $(C_5Me_5)_3Ln$ series, the yttrium complex displays the most extreme structural parameters. The 4.34-Å ring centroid–ring centroid distance is the smallest of the series (Table 7) and shows that these three rings can be located closer together than was observed in $(C_5Me_5)_3Sm$ and $(C_5Me_5)_3Gd$. $(C_5Me_5)_3Y$ also has the largest M–C bond distances in this series when differences in ionic radii are taken into account.

Recently, an analysis of the bending of the methyl groups out of the plane of the cyclopentadienyl ring in sterically crowded $(C_5Me_5)_3M$ complexes was published (29). This analysis shows that, although there is a large range in the out-of-plane displacement distances for the methyl groups in any specific complex, the most extreme value, the largest out-of-plane displacement, is the most diagnostic for unusual $(C_5Me_5)^{1-}$ reactivity. The $(C_5Me_5)_3M$ complexes that display unusual $(C_5Me_5)^{1-}$ reactivity have maximum out-of-plane displacements of 0.48 Å or greater. The out of plane methyl displacements in **3** (0.18, 0.36, and 0.55 Å) and in **5** (0.19, 0.39, 0.55 Å) fit this pattern. The 0.55-Å maximum displacements for **3** and **5** are consistent with the high reactivity of their $(C_5Me_5)^{1-}$ rings. Because **3** and **5** have the same maximum methyl displacements within experimental error, this metrical parameter does not distinguish the relative steric crowding in each.

Reactivity. The reactivity of $(C_5Me_5)_3Gd$ vis-à-vis $(C_5Me_5)_3Sm$ was of interest to determine whether the sterically more crowded complex of the smaller metal would have higher reactivity. Previously, it had been observed that the larger metals, La–Nd, which generate the less sterically crowded complexes, are less reactive than Sm (8). However, because Sm often has special reactivity because of the presence of its divalent state, Sm^{2+} (2, 11, 12), it was important to examine the metal size/reactivity relationship with both larger and smaller metals.

The reactivity of $(C_5Me_5)_3Gd$ with C_8H_8 and $Ph_3P=Se$ is similar to that of $(C_5Me_5)_3Sm$. One difference in the Gd chemistry is that 2 equiv of $(C_5Me_5)_3Gd$ readily react with 1 equiv of $Ph_3P=Se$ to give the unsolvated $[(C_5Me_5)_2Gd]_2(\mu-Se)$. With the larger metal, Sm, the unsolvated Se^{2-} complex did not readily crystallize; i.e., the product was only isolated as the THF adduct, $[(C_5Me_5)_2Sm(THF)]_2Se$. Overall, with the substrates examined, $(C_5Me_5)_3Gd$ has reactivity equal to that of Sm, and the correlation of size with reactivity is supported for metals both larger and smaller than Sm.



Scheme 5.

The chemistry of $(C_5Me_5)_3Y$ has an added dimension of being a powerful metalation reagent. $(C_5Me_5)_3Y$ is sufficiently reactive that it can metalate arene rings in a reaction that is contrary to the pK_a values of the participants (30). This high metalation reactivity for a normally inert $(C_5Me_5)^{1-}$ ligand is likely a consequence of the high steric crowding in $(C_5Me_5)_3Y$. Examination of the thermodynamics of this process compared with the data known on organolanthanides (31) suggests that the bond strength of one $(C_5Me_5)^{1-}$ ligand in a $(C_5Me_5)_3Ln$ complex is not much different from that of an aryl or benzyl ligand. This bond strength is much less than normally expected for a penta-hapto anion.

Conclusion

$(C_5Me_5)_3Ln$ complexes can now be made with lanthanide metals ranging in size from La to Y. All of these complexes have Ln–C(C_5Me_5) distances that are longer than conventional Ln– C_5Me_5 complexes and display $(C_5Me_5)^{1-}$ reactivity not observed in conventional pentamethylcyclopentadienyl lanthanide complexes. Hence, reactivity is observed that is consistent with access to intermediates like $(C_5Me_5)_2Ln(\eta^1-C_5Me_5)$ and SIR with $(C_5Me_5)^{1-}$ functioning as a reductant. The reactivity is variable depending on the degree of steric crowding across the range of metals, La–Y. This work shows that there is yet another type of reactivity available to $(C_5Me_5)_3Ln$ when steric crowding is severe enough, namely C–H activation. This type of reaction has not been described previously for the $(C_5Me_5)^{1-}$ ligand and shows how much the chemistry of a ligand can be changed by steric manipulation.

The fact that SIR chemistry can now be done with metals from La to Y means that size optimization of this reductive chemistry is possible. Variation in metal size should allow optimization of

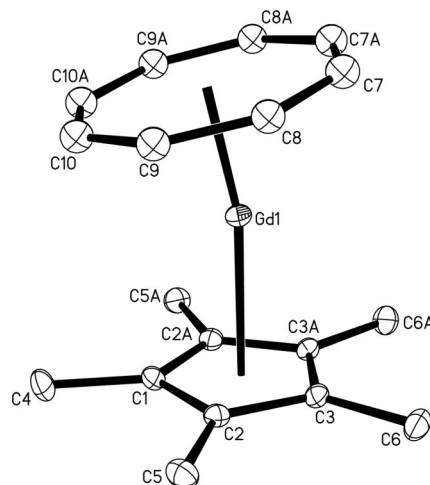
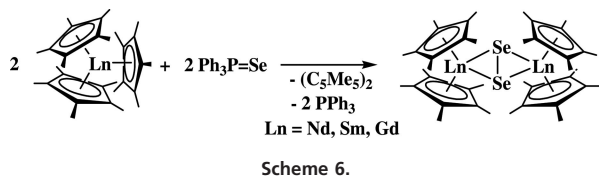


Fig. 4. Thermal ellipsoid plot of $(C_5Me_5)Gd(C_8H_8)$, **6**, with ellipsoids drawn at the 50% probability level.

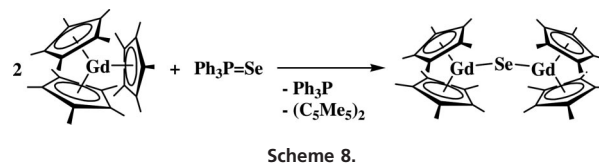
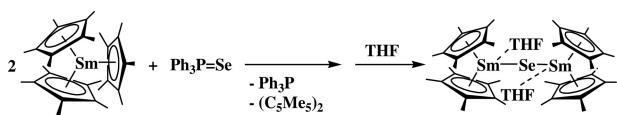


reaction rates, crystallinity of products, and selection of metal physical properties in a way that was not possible with the Sm^{2+} reductive chemistry of $(\text{C}_5\text{Me}_5)_2\text{Sm}$. Of particular interest is the fact that $(\text{C}_5\text{Me}_5)_3\text{Ln}$ complexes of both large and small diamagnetic compounds can be obtained, and the reaction chemistry of this class of long-bond organometallics can be studied in detail by NMR spectroscopy.

Materials and Methods

The syntheses and manipulations of these extremely air- and moisture-sensitive compounds were conducted under nitrogen or argon with rigorous exclusion of air and water by Schlenk, vacuum line, and glovebox techniques. Glassware was treated with Siliclad (Gelest, Morrisville, PA) to avoid formation of oxide decomposition products. Because the $(\text{C}_5\text{Me}_5)_3\text{Ln}$ complexes can react with ethers (7), all manipulations involving these complexes were done under ether-free conditions. THF, diethyl ether, toluene, hexanes, and benzene were saturated with ultra-high purity-grade argon (Airgas, Radnor, PA) and dried by passage through drying columns (GlassContour, Irvine, CA). All deuterio-solvents (Cambridge Isotope Laboratories, Andover, MA) and dioxane were dried over NaK alloy and vacuum transferred before use. $(\text{C}_5\text{Me}_5)_2\text{LnCl}_2\text{K}(\text{THF})_2$ (where Ln is Gd, Y) were synthesized in a manner similar to that of $(\text{C}_5\text{Me}_5)_2\text{LnCl}_2\text{K}(\text{THF})_2$ (Ln is Ce, Nd, Sm) as described (32). TMF was synthesized by literature methods (33). Allylmagnesium chloride (2.0 M in THF; Aldrich, St. Louis, MO) was used as received. $[\text{Et}_3\text{NH}][\text{BPh}_4]$ was prepared as described (34). ^1H and ^{13}C NMR spectra were obtained on 400- and 500-MHz spectrometers (Bruker, Billerica, MA) at 25°C . IR analyses were acquired as thin films by using a ReactIR 1000 (Applied Systems, Inc., Millersville, MD) (35). Elemental analyses were performed by Analytische Laboratorien (Lindlar, Germany). X-ray crystallographic files are available in Data Set 1, which is published as supporting information on the PNAS web site.

$(\text{C}_5\text{Me}_5)_2\text{Gd}(\text{C}_3\text{H}_5)$, 1. $(\text{CH}_2\text{CHCH}_2)\text{MgCl}$ (1.35 ml of a 2.0 M solution in THF, 2.97 mmol) was added to a stirred white slurry of $(\text{C}_5\text{Me}_5)_2\text{GdCl}_2\text{K}(\text{THF})_2$ (1.71 g, 2.48 mmol) in 50 ml of toluene. The mixture immediately changed color to form a yellow solution. After 1 h, the solvent was removed by rotary evaporation to yield a bright yellow solid. This material was triturated with hot hexanes (50 ml) and then 2% dioxanes in hexanes (50 ml) and filtered through a coarse frit to yield an orange solution. After removal of the solvent, the yellow solid was dried under high vacuum (1×10^{-7} torr) for 24 h to remove coordinated THF. The resulting material was extracted with hexanes and filtered to yield **1** (1.12 g, 94%) as a bright orange solid upon solvent removal. IR (thin film) 2907s, 2860s, 1540s, 1440s, 1378s, 1243s, 1023s, 722s cm^{-1} . Anal. Calcd. for $\text{C}_{23}\text{H}_{35}\text{Gd}$: C, 58.93; H, 7.54; Gd, 33.54. Found: C, 59.59; H, 7.45; Gd, 33.44



$(\text{C}_5\text{Me}_5)_2\text{Gd}[\text{BPh}_4]$, 2. Bright orange **1** (0.714 g, 1.52 mmol) and $[\text{Et}_3\text{NH}][\text{BPh}_4]$ (0.770 g, 1.82 mmol) were stirred in 40 ml of benzene for 4 h, and the mixture became an intense yellow slurry. The slurry was filtered, and **2** was washed through a frit by using warm benzene because it has low solubility in arenes. Crystallization from hot toluene, followed by washing with fresh toluene (2×10 ml) and hexanes (2×10 ml), yielded **2** as yellow needles (1.01 g, 88%). Anal. Calcd. for $\text{C}_{44}\text{H}_{50}\text{Gd}$: C, 71.79; H, 6.84; Gd, 21.36. Found: C, 71.08; H, 6.83; Gd, 21.90.

$(\text{C}_5\text{Me}_5)_3\text{Gd}$, 3. KC_5Me_5 (0.084 g, 0.485 mmol) was added to **2** (0.329 g, 0.441 mmol) in 15 ml of benzene, and the mixture was stirred for 24 h. Insoluble materials were removed by centrifugation, and the solvent was removed from the resulting red solution by rotary evaporation to yield **3** (0.141 g, 57%) as a dark red solid. IR (thin film) 2961s, 2907s, 2856s, 1440s, 1378s, 1258s, 1023s, 803m, 730m cm^{-1} . Anal. Calcd. for $\text{C}_{30}\text{H}_{45}\text{Gd}$: C, 64.00; H, 8.07; Gd, 27.93. Found: C, 64.13; H, 7.96; Gd, 28.10. Single crystals suitable for x-ray diffraction were obtained by cooling a hot toluene solution to RT.

$(\text{C}_5\text{Me}_5)_2\text{Y}[(\mu\text{-Ph})_2\text{BPh}_2]$, 4. $[\text{Et}_3\text{NH}][\text{BPh}_4]$ (0.193 g, 0.454 mmol) was added to a stirred solution of $(\text{C}_5\text{Me}_5)_2\text{Y}(\text{C}_3\text{H}_5)$ (ref. 36; 0.145 g, 0.303 mmol) in 10 ml of toluene. The intense yellow slurry quickly changed color to form a white slurry. After 4 h, centrifugation of the mixture left white insolubles. The insoluble material was extracted with 15 ml of benzene, and the mixture was filtered, leaving a clear and colorless solution. Removal of benzene *in vacuo* yielded **4** as a white solid (0.212 g, 92%). ^1H NMR (C_6D_6): δ 7.80 (b s, *m*- C_6H_5 , 8H), 7.23 (t, $J_{\text{HH}} = 7.2$ Hz, *o*- C_6H_5 , 8H), 7.10 (t, $J_{\text{HH}} = 7.2$ Hz, *p*- C_6H_5 , 4H), 1.62 (s, C_5Me_5 , 30H). ^{13}C NMR 139.0 (B(C_6H_5)₄), 131.4 (B(C_6H_5)₄), 128.4 (B(C_6H_5)₄), 127.6 (B(C_6H_5)₄), 122.5 (C_5Me_5), 11.4 (C_5Me_5). IR (thin film) 3057s, 2991m, 2968m, 2910s, 1590s, 1475s, 1432s, 1382m, 1332m, 1262s, 1243m, 1185m, 1154m, 1092m, 1061m, 1031m, 845s, 810s cm^{-1} . Anal. Calcd for $\text{C}_{44}\text{H}_{50}\text{YB}$: C, 77.87; H, 7.44; B, 1.59; Y, 13.10. Found: C, 76.76; H, 7.29; B, 1.50; Y, 13.22.

$(\text{C}_5\text{Me}_5)_2\text{Y}(\text{CH}_2\text{C}_6\text{H}_5)$ from 4. **4** (0.058 g, 0.075 mmol) and KC_5Me_5 (0.017 g, 0.097 mmol) were mixed together in 10 ml of toluene. After a few hours, the slurry became orange. After 12 h of stirring, a deep orange solution was separated from the insoluble material by centrifugation. Removal of the solvent yielded the orange solid

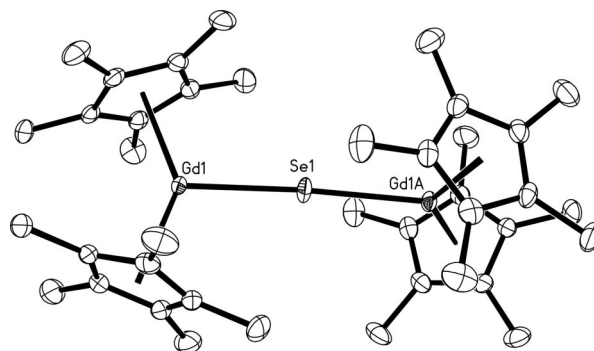
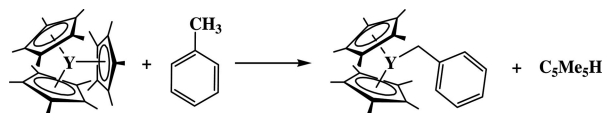


Fig. 5. Thermal ellipsoid plot of $(\text{C}_5\text{Me}_5)_2\text{Gd}]_2(\mu\text{-Se})$, **8**, with ellipsoids drawn at the 50% probability level.



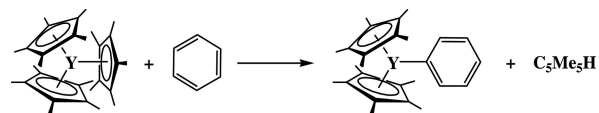
Scheme 9.

$(C_5Me_5)_2Y(CH_2C_6H_5)$ (0.029 g, 86%) identified by 1H NMR spectroscopy in C_6D_{12} (20). To further confirm the presence of $(C_5Me_5)_2Y(CH_2C_6H_5)$, this product was placed under an atmosphere of H_2 . The resulting spectrum matched that reported for $[(C_5Me_5)_2YH]_2$ (22).

$(C_5Me_5)_3Y$, **5**. $[(C_5Me_5)_2YH]_2$ (0.349 g, 0.484 mmol) was combined with yellow TMF (0.130 g, 0.968 mmol) in 10 ml of cyclohexane. An orange solution immediately resulted. Within 5 min, a precipitate formed. After 30 min of stirring, the volatiles were removed *in vacuo* to yield **5** (0.388, 81%) as an orange powder. 1H NMR (C_6D_{12}) δ 1.97. ^{13}C NMR (C_6D_{12}) δ 122.1 (C_5Me_5), 13.29 (C_5Me_5). IR (thin film) 2960s, 2910s, 2855s, 1478s, 1440s, 1380s, 1250s, 1154s, 1032s, 946m, 925m, 715s, 674m cm^{-1} . Anal. Calcd for $YC_{30}H_{45}$: Y, 17.97; C, 72.85; H, 9.17. Found: Y, 18.08; C, 72.67; H, 9.08. Single crystals suitable for x-ray diffraction formed in an NMR tube scale reaction with C_6D_{12} as the solvent. Low-temperature 1H NMR spectroscopy on $(C_5Me_5)_3Y$ using C_7D_{14} showed no change down to 188 K.

$(C_5Me_5)_2Y(C_6H_5)$ from **5**. $(C_5Me_5)_3Y$ (3 mg, 0.006 mmol) and C_6H_6 (5 mg, 0.061 mmol) were combined in C_6D_{12} . Initially, the 1H NMR spectrum indicated no reaction (1.97 and 7.21 ppm). However, after 1 day, the 1.97 ppm resonance began to diminish, and a new set of resonances began to appear, corresponding to $(C_5Me_5)_2Y(C_6H_5)$ (20). After 5 days at RT, 85% conversion was achieved.

$(C_5Me_5)_2Y(CH_2C_6H_5)$ from **5**. $(C_5Me_5)_3Y$ (6 mg, 0.012 mmol) and C_7H_8 (8 mg, 0.087 mmol) were combined in C_6D_{12} . After 1 h, the 1.97-ppm resonance was absent, and a new set of resonances was observed corresponding to $(C_5Me_5)_2Y(CH_2C_6H_5)$ (20). After 1 day at RT, 90% conversion was achieved.



Scheme 10.

$(C_5Me_5)Gd(C_8H_8)$, **6**. C_8H_8 (0.026 g, 0.251 mmol) and **3** (0.141 g, 0.251 mmol) were stirred at RT for 24 h in 10 ml of toluene. Even though no color change was observed, cooling the red solution to $-30^\circ C$ resulted in the formation of yellow crystals identified by x-ray diffraction as $(C_5Me_5)Gd(C_8H_8)$. The complex was isomorphous with the five other known analogs (25, 26).

$[(C_5Me_5)_2Gd]_2(\mu-\eta^2-\eta^2-Se_2)$, **7**. Within 5 min of addition of $Ph_3P=Se$ (0.121 g, 0.355 mmol) to **3** (0.200 g, 0.355 mmol) in 10 ml of toluene, the slurry changed from dark red to a bright orange and then back to a dark red. After 24 h, a yellow slurry was present and was centrifuged. The resulting red solids were washed with fresh toluene to yield **5** (0.073 g, 41%) identified by x-ray crystallography. The complex is isomorphous with the La, Nd, and Sm analogs (24, 27).

$[(C_5Me_5)_2Gd]_2(\mu-Se)$, **8**. Within 5 min of addition of $Ph_3P=Se$ (0.067 g, 0.197 mmol) to **3** (0.222 g, 0.394 mmol) in 10 ml of toluene, the slurry changed from dark red to bright orange and then to a luminescent yellow. After 24 h, the yellow slurry was centrifuged, and the yellow solution was evacuated to dryness. The product was extracted with hexane, and **6** was crystallized from cold hexanes as irregular yellow crystals (0.090 g, 49%) identified by x-ray crystallography. The complex is isomorphous with the Yb and Sm analogs (7, 28). IR (thin film) 2922s, 2856s, 1602m, 1451m, 1262s, 1092s, 1019s, 803s, 695s cm^{-1} .

X-Ray Data Collection, Structure Determination, and Refinement. For details on x-ray data collection, structure determination, and refinement for compounds **3–8**, see *Supporting Materials and Methods*, which is published as supporting information on the PNAS web site.

This work was supported by the National Science Foundation.

- Davies, C. E., Gardiner, I. M., Green J. C., Green M. L. H., Hazel, N. J., Grebenik, P. D., Mtetwa, V. S. B. & Prout, K. (1985) *J. Chem. Soc. Dalton Trans.*, 669–683.
- Evans, W. J. & Davis, B. L. (2002) *Chem. Rev.* **102**, 2119–2136.
- Evans, W. J., Gonzales, S. L. & Ziller, J. W. (1991) *J. Am. Chem. Soc.* **113**, 7423–7424.
- Evans, W. J. & Foster, S. E. (1992) *J. Organomet. Chem.* **433**, 79–94.
- Evans, W. J., Forrestal, K. J. & Ziller, J. W. (1995) *J. Am. Chem. Soc.* **117**, 12635–12636.
- Evans, W. J., Forrestal, K. J. & Ziller, J. W. (1997) *Angew. Chem. Int. Ed. Engl.* **36**, 774–776.
- Evans, W. J., Forrestal, K. J. & Ziller, J. W. (1998) *J. Am. Chem. Soc.* **120**, 9273–9282.
- Evans, W. J., Perotti, J. M., Kozimor, S. A., Champagne, T. M., Davis, B. L., Nyce, G. W., Fujimoto, C. H., Clark, R. D., Johnston, M. A. & Ziller, J. W. (2005) *Organometallics* **24**, 3916–3931.
- Evans, W. J., Hughes, L. A. & Hanusa, T. P. (1984) *J. Am. Chem. Soc.* **106**, 4270–4272.
- Evans, W. J. (2000) *Coord. Chem. Rev.* **206–207**, 263–283.
- Evans, W. J. (1987) *Polyhedron* **6**, 803–835.
- Evans, W. J. (2002) *J. Organomet. Chem.* **647**, 2–11.
- Evans, W. J. (1985) *Adv. Organomet. Chem.* **24**, 131–177.
- Anwander, R. & Herrmann, W. A. (1996) *Top. Curr. Chem.* **179**, 1–32.
- Shannon, R. D. (1976) *Acta Crystallogr. A* **32**, 751–767.
- Evans, W. J. (2002) *J. Organomet. Chem.* **652**, 61–68.
- Evans, W. J., Davis, B. L. & Ziller, J. W. (2001) *Inorg. Chem.* **40**, 6341–6348.
- Evans, W. J., Seibel, C. A. & Ziller, J. W. (1998) *J. Am. Chem. Soc.* **120**, 6745–6752.
- Tilley, T. D., Andersen, R. A., Spencer, B., Ruben, H., Zalkin, A. & Templeton, D. H. (1980) *Inorg. Chem.* **19**, 2999–3003.
- Booij, M., Deelman, B. J., Duchateau, R., Postma, D. S., Meetsma, A. & Teuben, J. H. (1993) *Organometallics* **12**, 3531–3540.
- Ringelberg, S. N., Meetsma, A., Troyanov, S. I., Hessen, B. & Teuben, J. H. (2002) *Organometallics* **21**, 1759–1765.
- den Haan, K. H., Wielstra, Y. & Teuben, J. H. (1987) *Organometallics* **6**, 2053–2060.
- Deelman, B. J., Booij, M., Meetsma, A., Teuben, J. H., Kooijman, H. & Spek, A. L. (1995) *Organometallics* **14**, 2306–2317.
- Evans, W. J., Nyce, G. W., Clark, R. D., Doedens, R. J. & Ziller, J. W. (1999) *Angew. Chem. Int. Ed.* **38**, 1801–1803.
- Evans, W. J., Johnston, M. A., Clark, R. D. & Ziller, J. W. (2000) *J. Chem. Soc. Dalton Trans.* **10**, 1609–1612.
- Schumann, H., Kohn, R. D., Reier, F. W., Dietrich, A. & Pickardt, J. (1989) *Organometallics* **8**, 1388–1392.
- Evans, W. J. & Lee, D. S. (2005) *Can. J. Chem.* **83**, 375–384.
- Berg, D. J., Burns, C. J., Andersen, R. A. & Zalkin, A. (1989) *Organometallics* **8**, 1865–1870.
- Evans, W. J., Kozimor, S. A. & Ziller, J. W. (2005) *Inorg. Chem.* **44**, 7960–7969.
- Bordwell, F. G. & Bausch, M. J. (1983) *J. Am. Chem. Soc.* **105**, 6188–6189.
- Nolan, S. P., Stern, D. & Marks, T. J. (1989) *J. Am. Chem. Soc.* **111**, 7844–7853.
- Evans, W. J., Keyer, R. A. & Ziller, J. W. (1993) *Organometallics* **12**, 2618–2633.
- Jutzi, P., Heidemann, T., Neumann, B. & Stammler, H. G. (1992) *Synthesis*, 1096–1098.
- Evans, W. J., Johnston, M. A., Greci, M. A., Gummshheimer, T. S. & Ziller, J. W. (2003) *Polyhedron* **22**, 119–126.
- Evans, W. J., Johnston, M. A., Clark, R. D. & Ziller, J. W. (2000) *Inorg. Chem.* **39**, 3421–3423.
- Evans, W. J., Kozimor, S. A., Brady, J. C., Davis, B. L., Nyce, G. W., Seibel, C. A., Ziller, J. W. & Doedens, R. J. (2005) *Organometallics* **24**, 2269–2278.